






## Article

# Monitoring the Dynamic Changes in Vegetation Cover Using Spatio-Temporal Remote Sensing Data from 1984 to 2020

Sajjad Hussain <sup>1,†</sup>, Shujing Qin <sup>2,\*,†</sup> , Wajid Nasim <sup>3</sup> , Muhammad Adnan Bukhari <sup>3</sup> , Muhammad Mubeen <sup>1</sup>, Shah Fahad <sup>4</sup>, Ali Raza <sup>5</sup> , Hazem Ghassan Abdo <sup>6,7</sup> , Aqil Tariq <sup>8,9,\*</sup> , B. G. Mousa <sup>10</sup> , Faisal Mumtaz <sup>11</sup>  and Muhammad Aslam <sup>12</sup> 

- <sup>1</sup> Department of Environmental Sciences, COMSATS University Islamabad, Vehari Campus, Vehari 61100, Pakistan
  - <sup>2</sup> State Key Laboratory of Water Resources and Hydropower Engineering Science, Wuhan University, Wuhan 430072, China
  - <sup>3</sup> Department of Agronomy, University College of Agriculture and Environmental Sciences, The Islamia University of Bahawalpur (IUB), Bahawalpur 63100, Pakistan
  - <sup>4</sup> Department of Agronomy, The University of Haripur, Haripur 22620, Pakistan
  - <sup>5</sup> School of Agriculture Engineering, Jiangsu University, Zhenjiang 212013, China
  - <sup>6</sup> Geography Department, Faculty of Arts and Humanities, Damascus University, Damascus P.O. Box 30621, Syria
  - <sup>7</sup> Geography Department, Faculty of Arts and Humanities, University of Tartous, Tartous P.O. Box 2147, Syria
  - <sup>8</sup> Department of Wildlife, Fisheries and Aquaculture, College of Forest Resources, Mississippi State University, 775 Stone Boulevard, Stackwelly, MS 39762, USA
  - <sup>9</sup> State Key Laboratory of Information Engineering in Surveying, Mapping and Remote Sensing (LIESMARS), Wuhan University, Wuhan 430079, China
  - <sup>10</sup> Department of Mining and Petroleum Engineering, Faculty of Engineering, Al-Azhar University, Cairo 11884, Egypt
  - <sup>11</sup> State Key Laboratory of Remote Sensing Sciences, Aerospace Information Research Institute, Chinese Academy of Sciences, Beijing 100101, China
  - <sup>12</sup> School of Computing Engineering and Physical Sciences, University of West of Scotland, Paisley G72 0LH, UK
- \* Correspondence: shujing.qin@whu.edu.cn (S.Q.); aqiltariq@whu.edu.cn (A.T.)  
† These authors contributed equally to this work.



**Citation:** Hussain, S.; Qin, S.; Nasim, W.; Bukhari, M.A.; Mubeen, M.; Fahad, S.; Raza, A.; Abdo, H.G.; Tariq, A.; Mousa, B.G.; et al. Monitoring the Dynamic Changes in Vegetation Cover Using Spatio-Temporal Remote Sensing Data from 1984 to 2020. *Atmosphere* **2022**, *13*, 1609. <https://doi.org/10.3390/atmos13101609>

Academic Editors: Xiangjin Shen, Binhui Liu and Graziano Coppola

Received: 18 July 2022

Accepted: 23 September 2022

Published: 30 September 2022

**Publisher's Note:** MDPI stays neutral with regard to jurisdictional claims in published maps and institutional affiliations.



**Copyright:** © 2022 by the authors. Licensee MDPI, Basel, Switzerland. This article is an open access article distributed under the terms and conditions of the Creative Commons Attribution (CC BY) license (<https://creativecommons.org/licenses/by/4.0/>).

**Abstract:** Anthropogenic activities and natural climate changes are the central driving forces of global ecosystems and agriculture changes. Climate changes, such as rainfall and temperature changes, have had the greatest impact on different types of plant production around the world. In the present study, we investigated the spatiotemporal variation of major crops (cotton, rice, wheat, and sugarcane) in the District Vehari, Pakistan, from 1984 to 2020 using remote sensing (RS) technology. The crop identification was pre-processed in ArcGIS software based on Landsat images. After pre-processing, supervised classification was used, which explains the maximum likelihood classification (MLC) to identify the vegetation changes. Our results showed that in the study area cultivated areas under wheat and cotton decreased by almost 5.4% and 9.1% from 1984 to 2020, respectively. Vegetated areas have maximum values of NDVI (>0.4), and built-up areas showed fewer NDVI values (0 to 0.2) in the District Vehari. During the Rabi season, the temperature was increased from 19.93 °C to 21.17 °C. The average temperature was calculated at 34.28 °C to 35.54 °C during the Kharif season in the District Vehari. Our results showed that temperature negatively affects sugarcane, rice, and cotton crops during the Rabi season, and precipitation positively affects sugarcane, rice, and cotton crops during the Kharif season in the study area. Accurate and timely assessment of crop estimation and relation to climate change can give very useful information for decision-makers, governments, and planners in formulating policies regarding crop management and improving agriculture yields.

**Keywords:** climate change; GIS; normalized difference vegetation index; Southern Punjab; remote sensing

## 1. Introduction

Climate change has the greatest effects on agriculture directly or indirectly worldwide [1–3]. The average global temperature has changed by 0.85 °C during the last 40 years all over the world due to anthropogenic activities [4–7]. Environmental and climatic changes have harmful effects on the vegetation cover in the following ways: changes in the temperature and rainfall [8], extreme heat stress and flash floods, variations in the disease vectors, and also the transfer of the people from rural to urban regions [9–12]. Additionally, economic and demographic factors can play an important role in changes in climate and vegetation cover [13–16]. Therefore, monitoring such intensification is significant for decision-making supports linked to food scarcity [17–19], overconsumption of water, health security, climate change mitigation, and adaptation. Furthermore, natural climatic drivers changed the atmospheric greenhouse gas, aerosol loading, and the properties of the Earth's surface, for example, volcanic eruptions, ocean currents, solar variations, topography, albedo, and vegetation cover, could change the local or even global climate [20–23].

Vegetation is a significant component of the terrestrial ecosystem and plays a significant role in the ecosystem's energy flow and material circulation [23,24]. Topography, climate, and human activities; together influenced the vegetation that creates feedback and adapting effects for human activities and climate [25–27]. The Normalized Difference Vegetation Index (NDVI) is an important indicator for identifying vegetation cover and is commonly used for identifying the relationship between climate change and various crops [28–31]. The NDVI has also been used for quantitative and qualitative assessment of vegetation cover and growth activity [32–35]. It also describes the health and greenness of different vegetation. Understanding the relation of climate factors with NDVI is critical for protecting environmental and natural resources [36]. Great attention had been paid to the relationship between temperature and vegetation. More research was essential to attain more extracted temperature and rainfall parameter accuracy [37], as well as to concentrate on the study of climate and vegetation change, to understand the ecological impact on urbanization and vice versa [38–40]. Monitoring cropping practices using remote sensing (RS) is an efficient tool on a global scale [41,42]. This is due to the increasing number of advanced civilian satellites and the high resolution of the onboard sensors. Humans' multiple cropping practices over the land surface can be monitored and captured by satellites at different temporal and spatial scales [43–47].

By the Global Climate Risk Index (GCRI) 2014, Pakistan was ranked 3<sup>rd</sup> amongst the worst climate-affected countries such as India, Bangladesh, etc. [48,49]. The heat wave was analyzed over various provinces of Pakistan (Baluchistan, Punjab, and Sindh) using historical data (1997–2015) to detect the maximum and minimum temperature tendencies [50]. Southern Punjab had a population of 29 million, while Punjab's total population at that time was 91 million [51,52]. This region lacks sufficient resources to support its people as most areas are undeveloped with weak infrastructure [53]. Presently, the most important problem built-up lands suffer from is the decreasing area of vegetation land caused by increasing temperature (non-transpiring and non-evaporating and ultimately change in land cover) [54,55]. According to Aslam et al. [56], almost 40 million people in Pakistan are under poverty stress; an estimated 10 million belong to the Southern Punjab region [57,58]. In the recent decade, there has been an upsurge in precipitation and temperature variation over Southern Punjab [59]. Vehari, one of the Multan divisions, is known as King of Cotton in Pakistan. According to Amin et al. [60], District Vehari has two agro-climatic zones categorized as low-intensity Punjab and cotton-wheat cropping zones. These agro-climatic zones are primarily based on changing climate patterns, crop rotation, and cropping patterns in District Vehari. Therefore, it is necessary to study the relationship of vegetation cover with climate change to improve vegetation cover and major crops in Southern Punjab, Pakistan. The important objectives of this research are to classify major cultivated crop changes from 1984 to 2020 using Landsat images in the District Vehari and to calculate the NDVI trend of cultivated crops and climate changes (temperature and rainfall) from 1984

to 2020. Additionally, we aim to show the relationship between climate change and major crops in the District Vehari.

## 2. Materials and Method

### 2.1. Study Area

The study area is District Vehari of Southern Punjab (Pakistan). This area lies between latitude  $29^{\circ}35'51''$  N to  $30^{\circ}22'21''$  N and longitude  $71^{\circ}43'54''$  E to  $72^{\circ}58'43''$  E approximately (Figure 1). Geographically, District Vehari was composed of productive land with semi-arid conditions. Months (June, July, and August) are the warmest months, with mean temperatures ranging from  $38^{\circ}\text{C}$  to  $48^{\circ}\text{C}$ . This area is irrigated through the water of rivers Ravi and Sutlej. The major crops of this area are wheat, rice, cotton, and sugarcane. The cropping pattern of District Vehari has 2 growing periods, named Rabi and Kharif seasons. Wheat and winter crops, mostly berseem (*Trifolium alexandrinum*), are grown in the Rabi season, whereas cotton, rice, and summer crops such as (maize and sorghum) are grown in the Kharif season. Rabi season starts in November and ends during April, as well as Kharif season from May to October. Sugarcane is a yearly crop frequently cultivated in September and February. Their study indicated that District Vehari had a drastic climate change. For example, very warm in summer (up to  $48.7^{\circ}\text{C}$ ) and very cold (up to  $1^{\circ}\text{C}$ ) in winter (Figure 2).

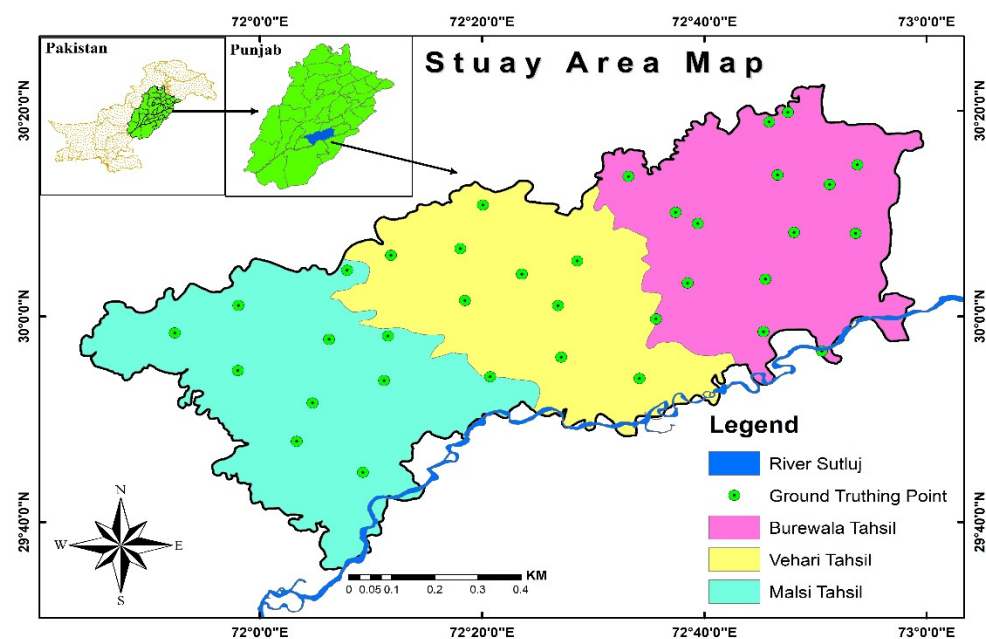


**Figure 1.** Geographical location of study area (Vehari).

### 2.2. Remote Sensing Data

Multispectral images from satellite observatory Landsat data were used to identify the cropping pattern of major crops. Landsat-based images with  $30\text{ m} \times 30\text{ m}$  spatial resolution were downloaded from the United States of Geological Survey (USGS) website (<https://earthexplorer.usgs.gov/> (accessed on 18 April 2021)) for the years 1984, 1993, 2002, 2011, and 2020, covering the study area. For this study, Landsat 5 Thematic Mapper (TM) for 1984 and 1993, Landsat 7 Enhanced Thematic Mapper Plus (ETM+) for 2002 and 2011, and Landsat 8, Operational Land Imager (OLI) for 2020 were used, as shown in Table 1. In this study, we also used Landsat 5, 7, and 8 satellite images for the NDVI and crop extraction of Rabi and Kharif seasons. The NDVI maps were prepared using Software Arc GIS 10.6 [61]. NDVI is also one of the most generally used vegetation indices and ranges from  $-1$  to  $1$  [62,63].

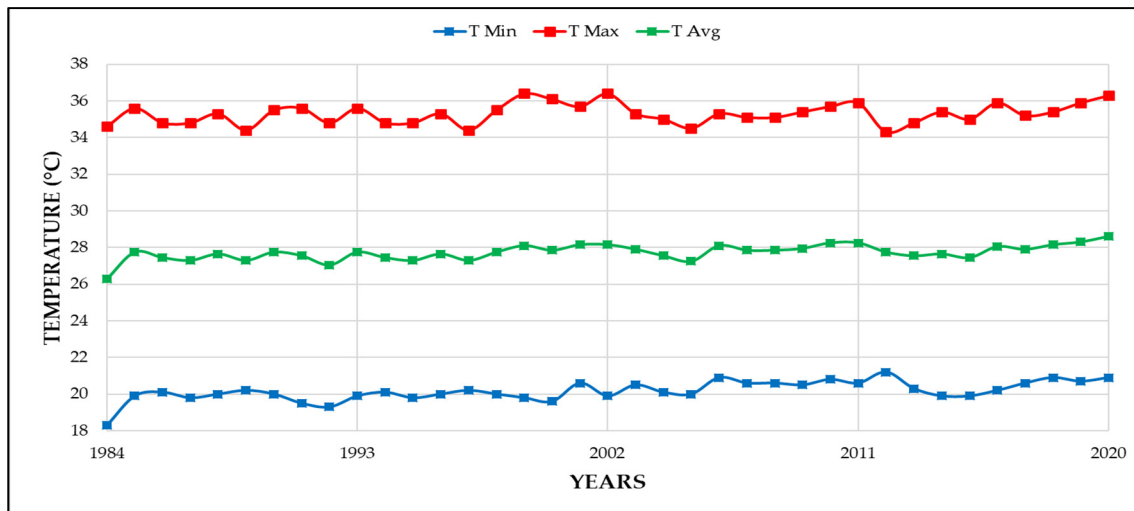


**Figure 2.** Mean maximum, minimum, and average temperature of the study area from 1984 to 2020.

**Table 1.** Specification of Landsat satellite images.

Satellite	Sensor	Spatial Resolution	Temporal Resolution	Paths	Row	Months	Years
Landsat 5	TM	30 m	16 days	149 and 150	39	March and September	1984 and 1993
Landsat 7	ETM+	30 m	16 days	149 and 150	39	March and September	2002 and 2011
Landsat 8	OLI	30 m	16 days	149 and 150	39	March and September	2020

*2.3. Climate Factor Data*

The rainfall, maximum and minimum temperature data were downloaded from the website (<http://power.larc.nasa.gov> (accessed on 12 June 2020)) of 20 different survey points of District Vehari from 1984 to 2020. The 3-year data sequence for all the survey points was analyzed by running a significant test at a 95% significant level to check the homogeneity of the data.

*2.4. Survey*

The survey was conducted in the districts of Vehari to collect information data about different crops and LULC changes. Overall, 20 union councils (UCs) were selected in District Vehari, and from each UC, 3 villages were selected for survey using the simple random technique (SRT). Therefore, a total of 60 surveys were conducted in the District Vehari.

*2.5. Image Classification and Analysis*

Landsat 5, 7, and 8 satellite images consist of different bands; 1 to 7 bands were used to classify major crops. The first step, atmospheric correction, layer stacking, and sub-setting, were analyzed using Landsat images based on the study area using ERDAS imagine software 2016 [64]. Atmospheric correction is the process of removing the effects of the atmosphere on the reflectance values of satellite images. These data processing steps must be completed to obtain a good quality result. Second step, crop pattern distribution maps were prepared using MLC classification and training site selections [65]. Spectral signatures resultant from the Landsat images were noted using the pixels enclosed by these polygons for the respective crop types [66,67]. To achieve crop classification, a supervised classification technique based on ground truthing was employed. Supervised classification was applied to Landsat images of 1984, 1993, 2002, 2011, and 2020 to generate classified crop maps. ERDAS Imagine and Arc GIS software are important for extracting different crops. A detailed methodology was presented in Figure 3.

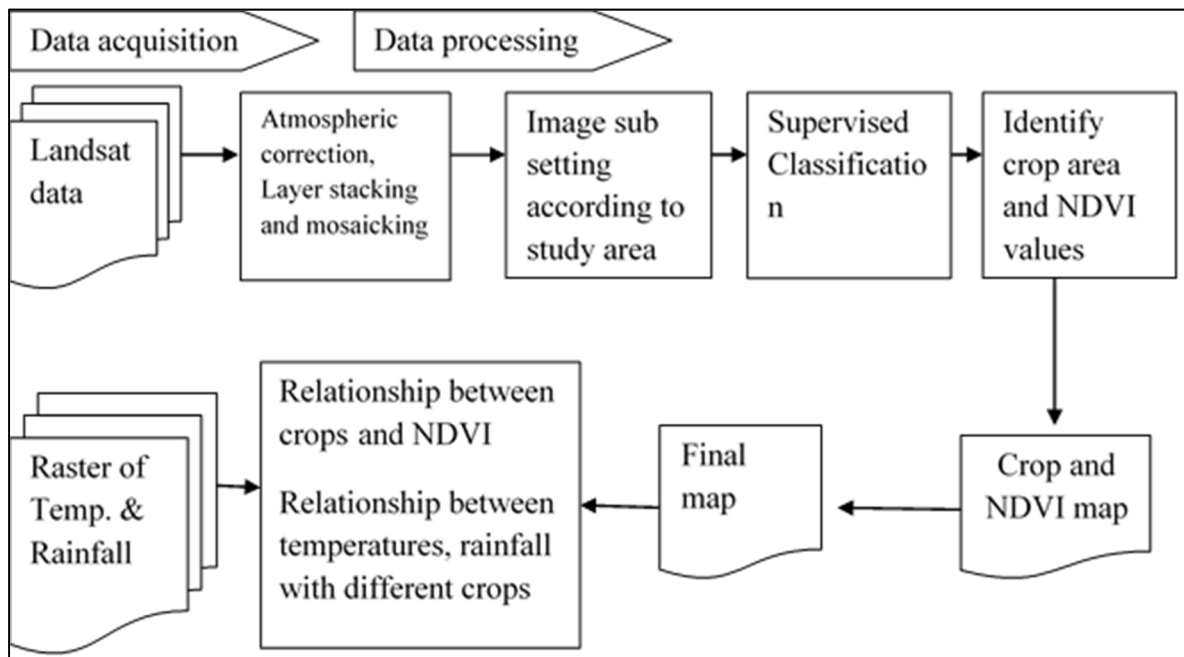


**Figure 3.** Flow chart for the methodology.

### 2.6. Trend and Correlation Analysis

Analysis of simple regression trend (SRT) was calculated using ArcGIS 10.6 and Microsoft Excel software. Software ArcGIS 10.6 was used to identify the NDVI characteristics. The slope trend was used to designate the NDVI changes in the study area by using Equation (1) [27].

$$\text{Slope} = \frac{n \times \sum_{i=1}^n i \text{NDVI}_i - \sum_{i=1}^n i \sum_{i=1}^n \text{NDVI}_i}{n \times \sum_{i=1}^n i^2 - (\sum_{i=1}^n i)^2} \quad (1)$$

where  $i$  shows the seasonal duration (days) such as Rabi and Kharif season;  $n$  is the monitoring year (like 1984 to 2020); NDVI means the mean values of NDVI for the studied year; slope change in NDVI over time for different seasons, if slope  $> 0$ , it shows NDVI trend is increasing in  $n$  years; otherwise, it is decreasing [68,69].

Rainfall and temperature affect NDVI; therefore, studying the relationship between climate factors and vegetation cover is necessary. Partial correlation analysis (PCA) permits that when 2 elements are concurrently connected to a 3rd variable, the effect of the 3rd element can be removed, and the relationship between the 2 elements is analyzed, which helps represent the relationship between NDVI and climate factors. For PCA calculation, the relationship between the 2 variables was calculated by using equation 2 [70,71]:

$$r_{xy} = \frac{\sum_{i=1}^n [(x_i - \bar{x})(y_i - \bar{y})]}{\sqrt{\sum_{i=1}^n (x_i - \bar{x})^2 \sum_{i=1}^n (y_i - \bar{y})^2}} \quad (2)$$

where  $r$  shows the relationship between  $x$  and  $y$  elements,  $x_i$  is the NDVI as well as  $y_i$  shows the temperature and rainfall,  $\bar{x}$  shows the mean values of NDVI, and  $\bar{y}$  shows the mean temperature and rainfall for the corresponding period in the study area.

## 3. Results

### 3.1. Change in Major Crops

Wheat and cotton were the main crops of the Rabi and Kharif seasons. Some other minor crops (rice, sugarcane, and vegetables) were grown in the study area. The Kharif

cropping period is from May to October (south-west monsoon), and the Rabi cropping period is from November–March (winter). The wheat area was presented at 64.7% and 59.3% in 1984 and 2020, respectively, in District Vehari (Figure 4). The wheat area decreased by almost 5.4% from 1984 to 2020 in the study area (Figure 5). The area of other crops was observed at 9.8% and 13.2% during 1984 and 2020, respectively, which increased by almost 3% from 1984 to 2020 during the Rabi season. The sugarcane area was observed at 17.3% and 15.3% during 1984 and 2020, respectively. The sugarcane area decreased by almost 2% from 1984 to 2020 in the Rabi season in the study area.

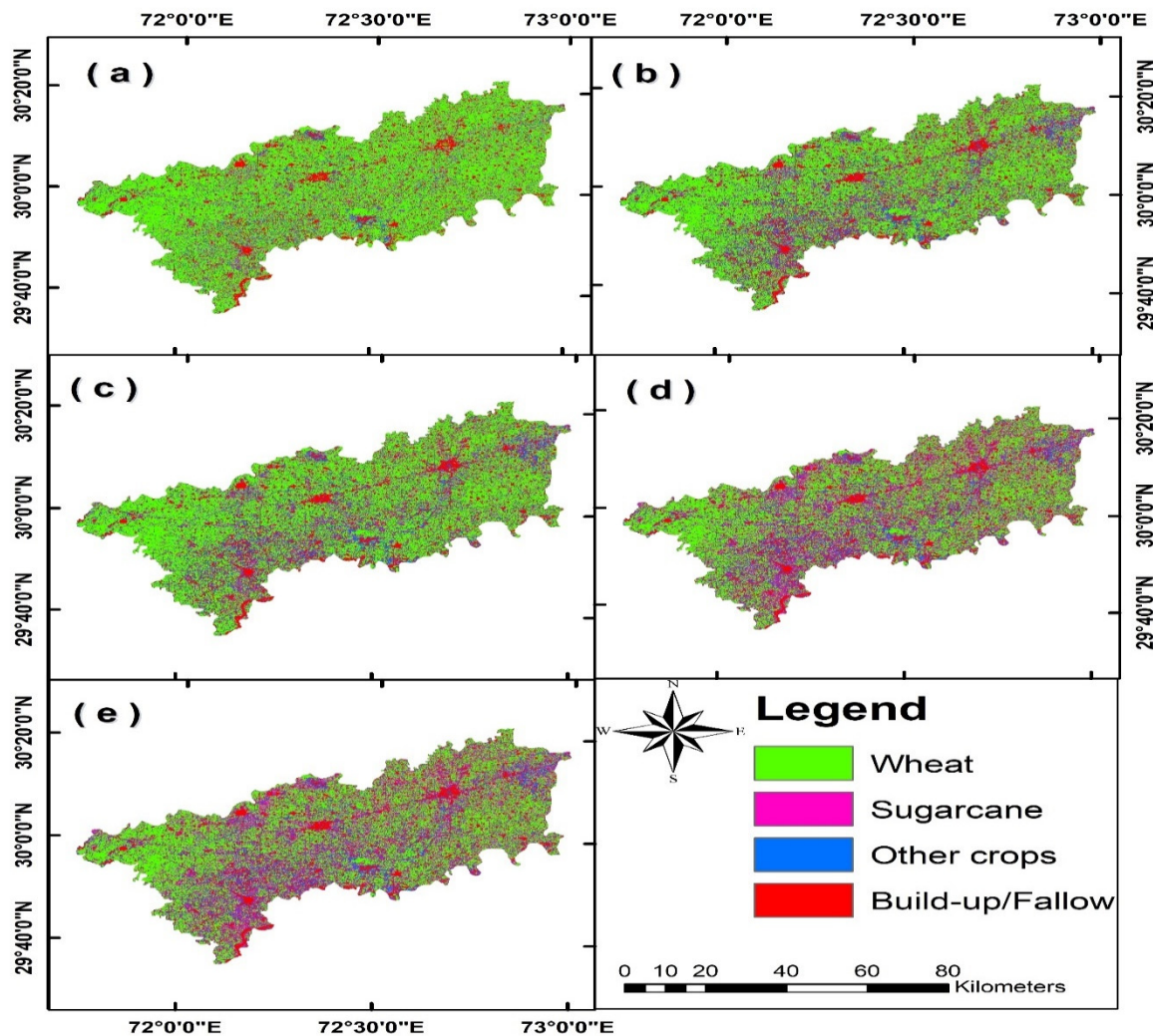


**Figure 4.** Crop identification map for Rabi season (a) 1984 (b) 1993 (c) 2002, (d) 2011 and (e) 2020.

In Kharif seasons, cotton was a key crop in District Vehari, with a total cropped land from 40.2% in 1984 to 31.1% in 2020. Cotton area decreased by 9.1% from 1984 to 2020 in District Vehari (Figure 6). The Rice area was observed to cover 14.3% and 18% during 1984 and 2020, respectively, in the study area. The cultivated area under rice increased by almost 4% from 1984 to 2020. Another crop area, maize, was observed at 16.5% and 26.8% between 1984 and 2020 in the Kharif season (Figure 7). In the study area, the sugarcane area was observed at 17.3% and 15.3% during 1984 and 2020, respectively. The cultivated area under sugarcane decreased by almost 2% from 1984 to 2020. The building/fallow land increased from 9.1% to 10.2% from 1984 to 2020 in the study area.

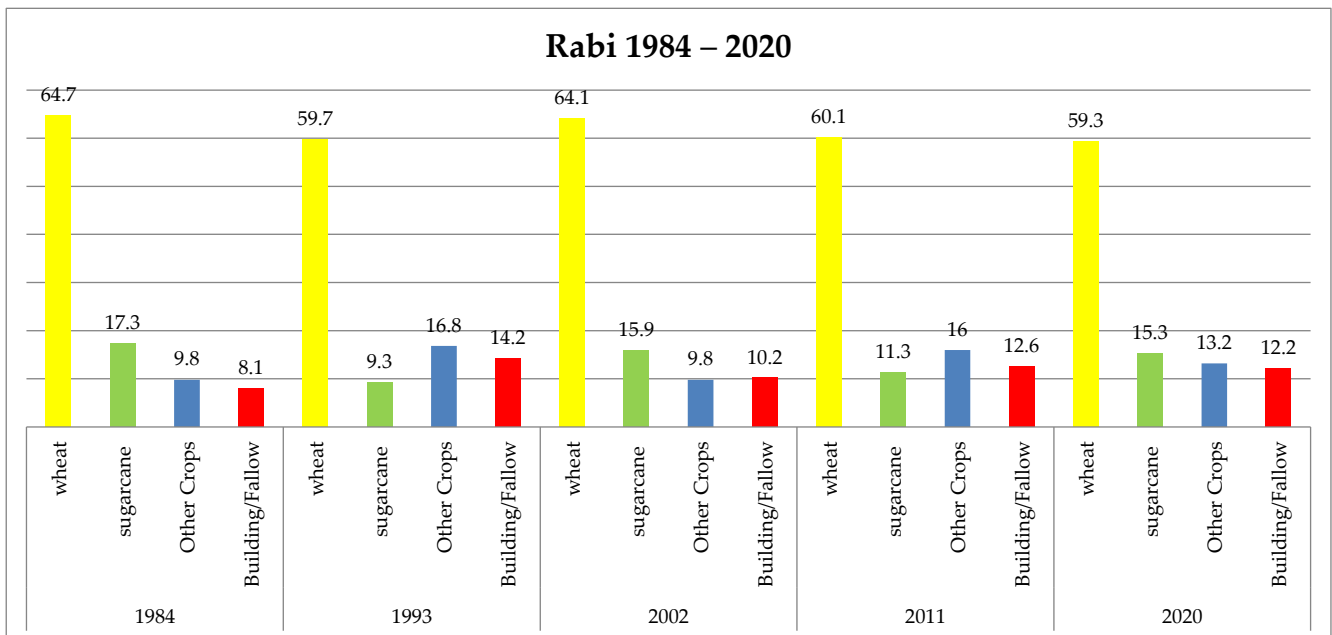


Figure 5. The cultivated area of major crops during Rabi seasons in District Vehari.

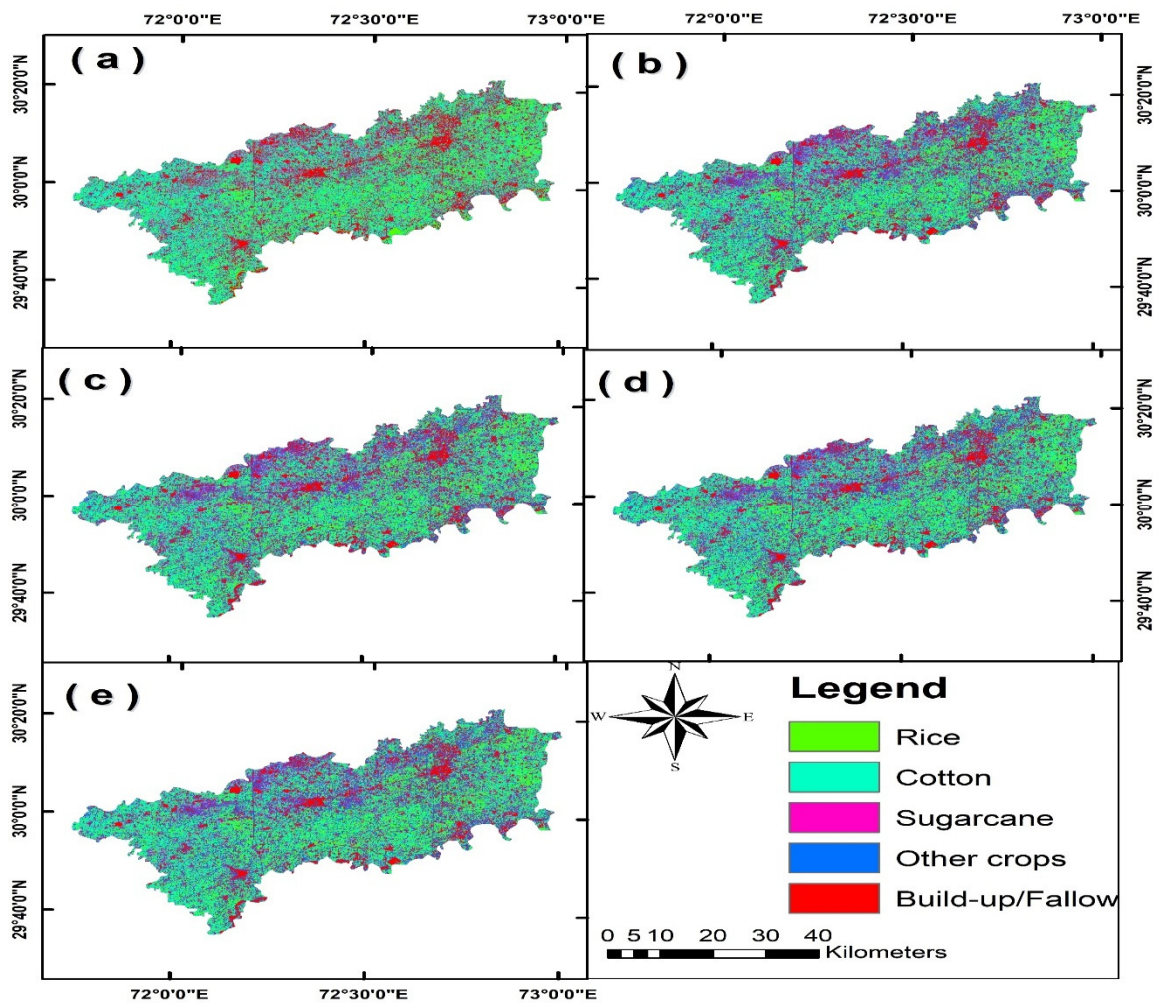


Figure 6. Crop identification map for Kharif season (a) 1984 (b) 1993 (c) 2002, (d) 2011 and (e) 2020.

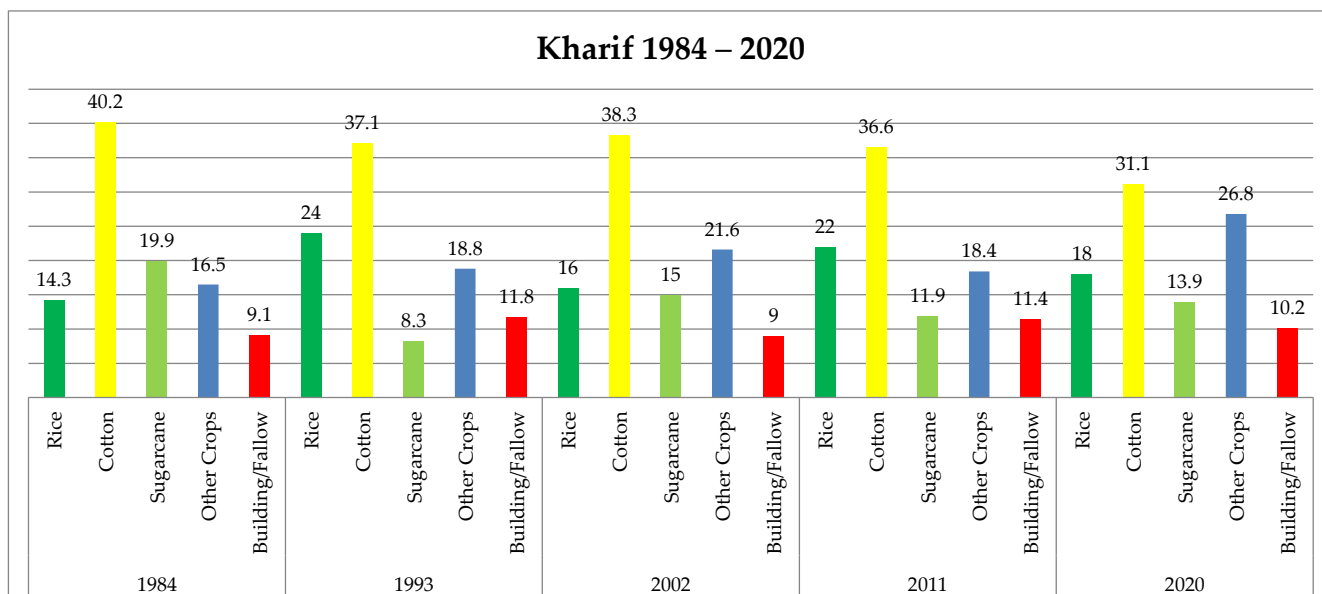


Figure 7. Cultivated are major crops during Kharif seasons in District Vehari.

### 3.2. Trend of NDVI for Different Crops

Figures 8 and 9 showed that total selected crops had slight increasing or decreasing trends of NDVI during the last 36 years. Mostly, the vegetation area has maximum values of NDVI from 0.4 to 0.6, and the built-up area shows fewer values of NDVI from 0 to 0.2. Wheat is the main crop of the Rabi season and is cultivated during November, while NDVI values become greatest during February in the study area (Figure 8). During the Rabi season, wheat had the maximum values of NDVI between 0.3 to 0.6, whereas the built-up area had the minimum NDVI values for 36 years. The NDVI values of Rabi fodder also decreased from 1984 to 2020. Our results showed a decreasing trend in the selected crop types during the Rabi season in the study area. This decrease in NDVI values is generally attributed to a decrease in vegetation greenness areas, especially cotton and wheat.

During the Kharif season, rice had maximum NDVI values (more than 0.6) in 1984. However, due to decreasing rainfall, the NDVI trend in rice decreased during 2020 in the study area. Sugarcane is regularly cultivated in February, and its NDVI trend remains low in the Rabi season and attains maximum values during the Kharif season due to increased vegetative growth. The NDVI trend of sugarcane had the same maximum NDVI as cotton, from 0.3 to 0.6. The NDVI trend of cotton showed the greatest NDVI values (more than 0.6) during all seasons in 1984, but this trend decreased in 2020 (Figure 9). Cotton mainly had fewer NDVI values, which may be mostly due to the dry and hot climate from 1984 to 2020. It is observed that the area with major crops decreased from 1984 to 2020 at a rate corresponding to the decreased rate of vegetation greening such as NDVI. The built-up area and barren land showed a similar trend of NDVI between (0.1 to 0.2) during the Rabi and Kharif seasons from 1984 to 2020.

### 3.3. Climate Factor of the Study Area

Climate change has the greatest influence on various crops in different portions of the biosphere [19,21]. Various climatic factors, such as temperature and rainfall, are more related to various crops. The rainfall and temperature data were collected from field surveys with coordinates such as latitude and longitude, fed to Arc GIS 10.6 software, and the maps were prepared. Figure 10 represents the average temperature maps of the Vehari district for the Rabi and Kharif seasons. During the Rabi season, the low temperature was noted as 19.93 °C, and the high temperature rises to 21.17 °C (Figure 10). It is observed that three survey points such as Chak 32 WB, Chak 1 WB, and Ludden, were calculated as the minimum temperature in the study area. Similarly, Tiba Sultan Pur and Chak Rasool Pura



were noted at maximum temperature. The average temperature was noted as 20.38 °C to 20.61 °C at Karampur during Rabi season in District Vehari. During the Kharif season, the low temperature was calculated to be 33.59 °C and the high temperature rises to 35.32 °C. It is clearly understood that Chak no 1WB was noted minimum temperature in the study area. Similarly, Tiba Sultan Pur and Chak Rasool Pura showed maximum temperature. The average temperature was calculated from 34.28 °C to 34.54 °C at Chak no 215 WB and Ludden during the Kharif season in District Vehari.

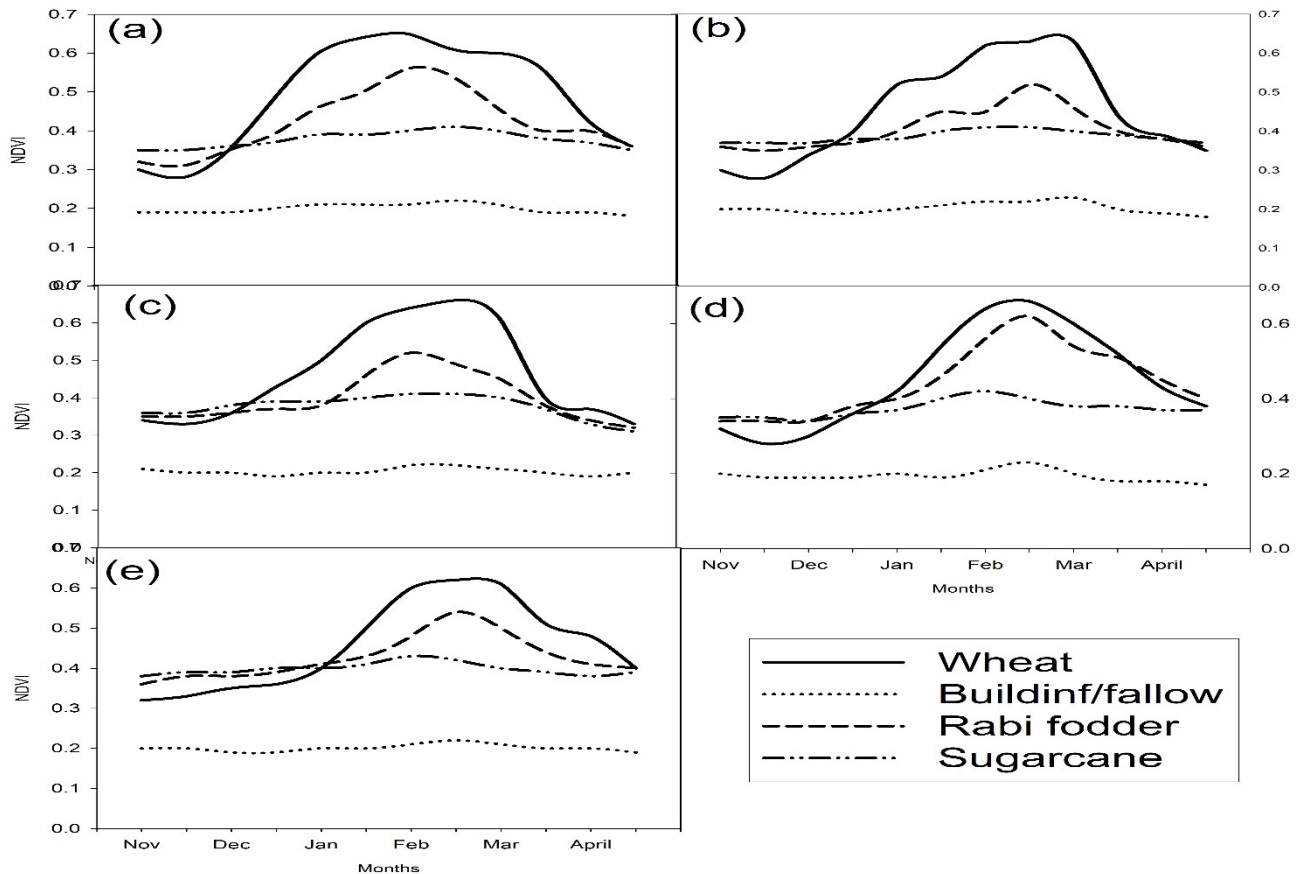


**Figure 8.** Mean NDVI seasonal changes for major crops during Rabi season (a) 1984, (b) 1993, (c) 2002, (d) 2011 and (e) 2020.

Figure 11 shows the average minimum and maximum precipitation for Rabi and Kharif seasons in District Vehari. During the Rabi season, the minimum precipitation value was noted at 39.50 mm, and maximum precipitation rises 87.32 mm. It is detected that Tiba Sultan Pur, Ludden, and Chak Rasool Pura were calculated as minimum precipitation. Similarly, Arain Wahan and Haji Shar recorded maximum rainfall in the study area. Average rainfall was noted from 60.50 mm to 66.69 mm at Karam Pur and Shaikh Fazal during the Rabi season in District Vehari. During the Kharif season, the maximum and minimum rainfall values were noted as 128.35 mm and 193.22, respectively. From the precipitation map, it is observed that Ludden and Arain Wahan calculated maximum rainfall. Similarly, Chak No. 1 WB, Chak No. 215 Wb, and Haji shar recorded minimum rainfall in the study area. Average rainfall was noted as 155–165 mm at Tiba Sultan Pur.

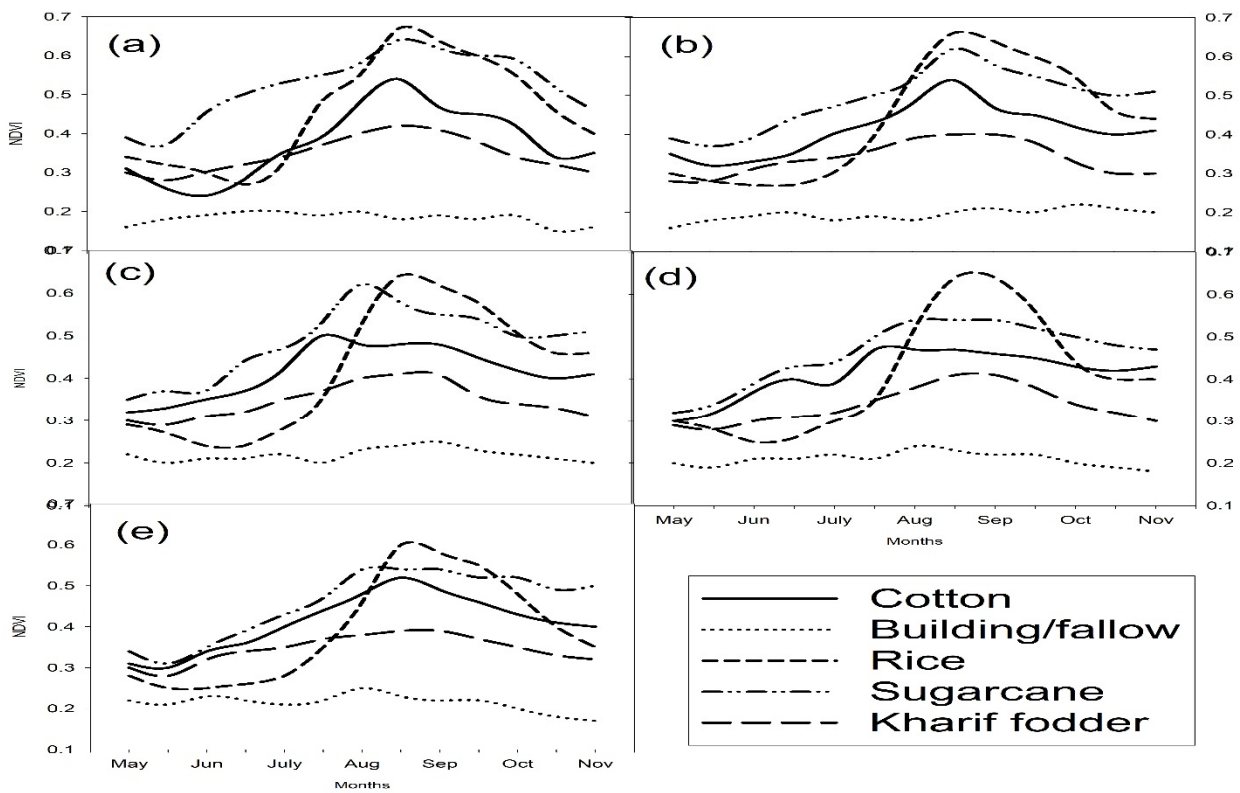


Figure 9. Mean NDVI seasonal changes for major crops during Kharif season (a) 1984, (b) 1993, (c) 2002, (d) 2011 and (e) 2020.

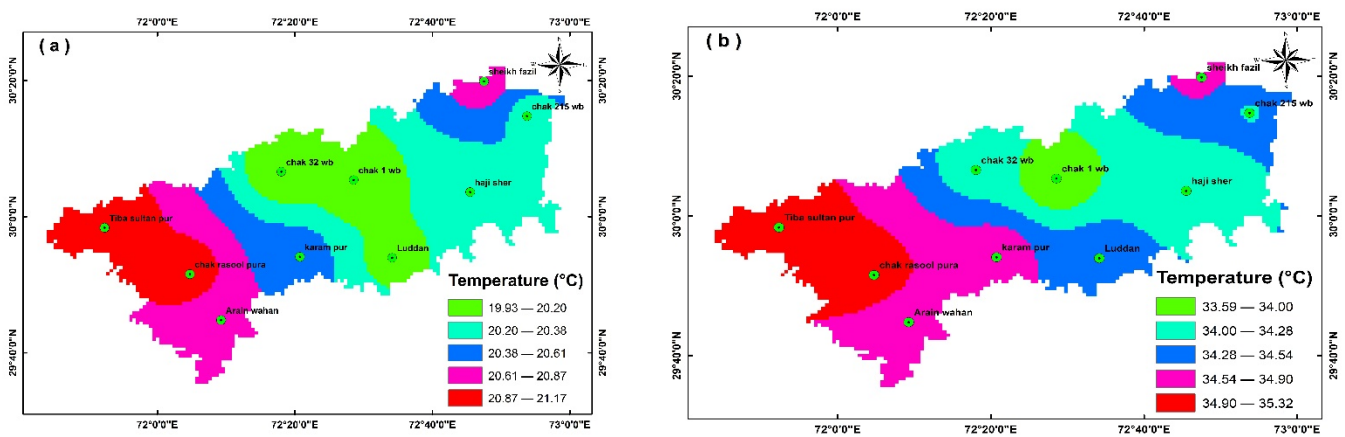


Figure 10. Maps of mean temperature during 1984 to 2020 (a) Rabi and (b) Kharif season.

### 3.4. Trend and Relation of Climate Factor with NDVI

Climate change significantly influences the flexibility of LULC classes in different portions of the environment. Furthermore, climate change influenced the terrestrial life strictly connected with hydrological cycles, thus affecting NDVI to a maximum amount [6].

Various climatic factors such as temperature and rainfall were linked with LULC. Wheat was the major crop in the study area and was sown from the last week of November onward. Comparatively, the high temperature was noted for wheat in the early stages with less precipitation during November. As a result, the NDVI values were very low at the sowing of wheat, for example, 0.2 (Figure 12). After this, temperature reduced, and precipitation increased during January and February, causing a rise in NDVI values (up to 0.6) of wheat growth. The temperature increased at the end of the wheat season, and NDVI values continued to reduce till its harvest during April. In short, climate change

positively affects rainfall, and temperature negatively affects wheat production in District Vehari. These environments are suitable for maximum wheat yield in District Vehari, as stated by local crop specialists, who believed that fewer temperatures during germination would suppress crop growth; however, higher temperatures in the middle stages (mainly in the milking step) would cause crop shriveling.

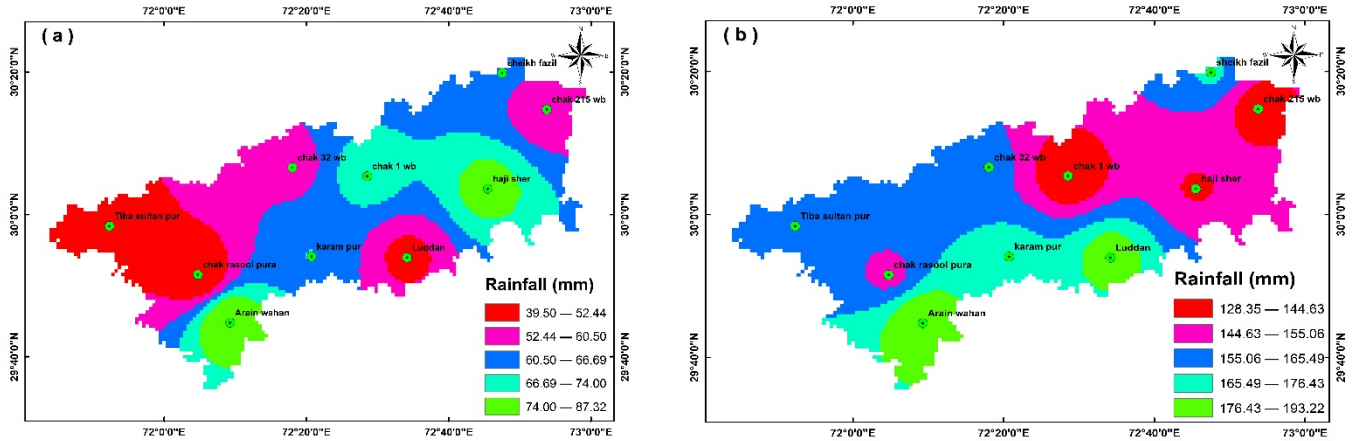


Figure 11. Maps of mean rainfall from 1984 to 2020 (a) Rabi and (b) Kharif season.

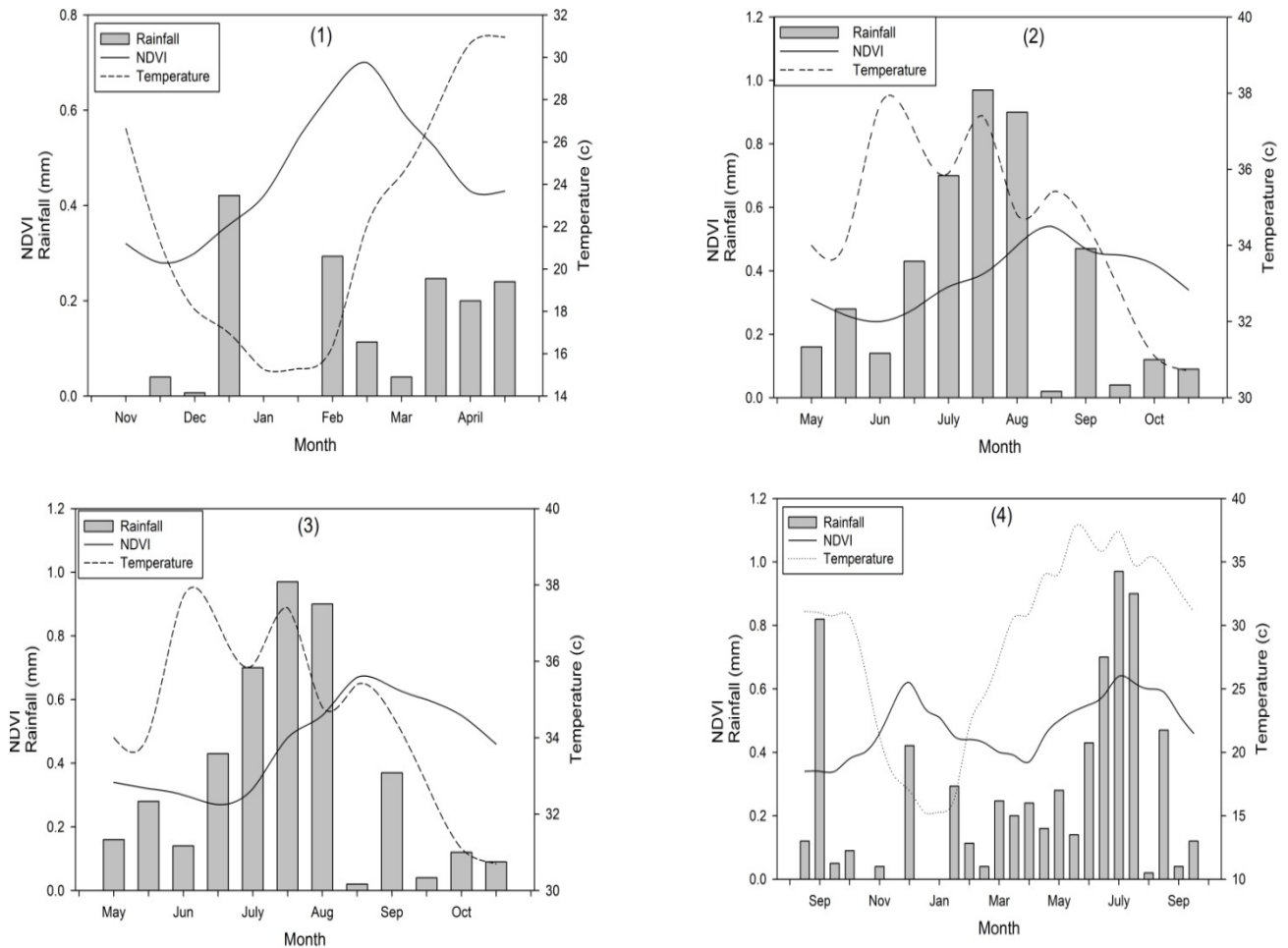


Figure 12. The trend of NDVI with rainfall and temperature is (1) wheat, (2) cotton, (3) rice, and (4) sugarcane.

Cotton is the second largest crop and is mostly sown in May in the study area. Comparatively, less temperature was noted for cotton in the early stages, with less precipitation during May. However, after this, temperature and rainfall increased during July and August, which is perfect for cotton cultivation. Similarly, NDVI values (up to 0.6) also increased during these months, which showed that this area is perfect for cotton cultivation (Figure 12). However, for a few years, rainfall decreased, which has the greatest impact on cotton in the study area. Therefore, the temperature trends for cotton crops in the Kharif season were not dissimilar and displayed less variation during the growing season; however, the main difference was noted in the case of precipitation.

Rice is the third largest crop and is mostly sown in June in the study area. In areas of rice growing, less precipitation occurs during the germination stages. After that, it increases, resulting in a rise in NDVI in the Kharif season graph (Figure 12). Monsoon rainfall, mostly in July, helps full rice growth. However, rainfall decreased during the last few years, affecting rice. Sugarcane is regularly cultivated in February, and its NDVI trend remains low in the Rabi season and attains maximum values during the Kharif season due to increased vegetative growth. The NDVI value was comparatively static in winter, mostly due to minimum temperature combined with less precipitation, suppressing sugarcane vegetative activity. During the Kharif season, NDVI values of sugarcane increased due to increased rainfall in July and August.

Climate change has affected vegetation cover worldwide [71]. Temperature and precipitation were increasingly related to vegetation cover. To detect the relationship between vegetation cover and climate factors, regression coefficients ( $R^2$ ) were completed in District Vehari. In our research, regression ( $R^2$ ) 0.8346 and 0.6658 were calculated for the temperature and rainfall, respectively (Figure 13). The regression  $R^2$  tendency indicated that NDVI and temperature were negatively connected. Similarly, our results showed that rainfall and NDVI were positively connected. Regression analysis presented that temperature must increase in such areas where NDVI decreased. Our results also showed that in such areas where rainfall increased, NDVI must increase in District Vehari. Analysis presented that the temperature was higher in the built-up area compared to vegetation areas and other land features. Areas with maximum NDVI values have been designated as having sufficient vegetation, which produces cooling effects, thereby decreasing the temperature in such areas. Our results also suggested that increasing the temperature in the growing season had a central effect on the vegetation dynamics.

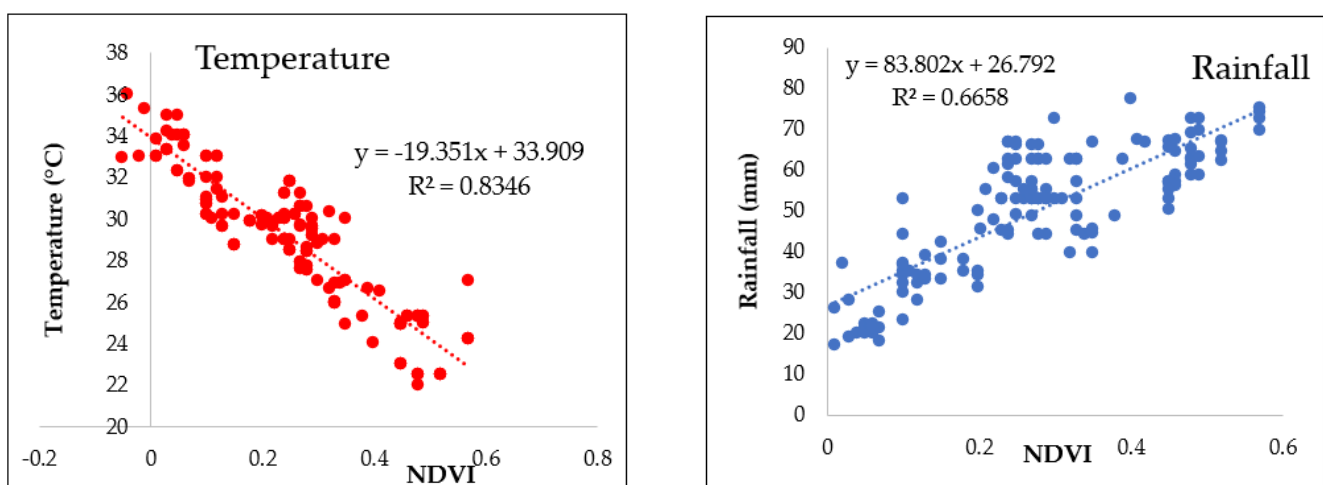


Figure 13. Relationship between NDVI with temperature and rainfall.

#### 4. Discussion

This study was utilized to examine the influence of climate change on major crops in Southern Punjab from 1984 to 2020 using Landsat images. Landsat images were used to classify the major crops most susceptible to environmental and climate changes. This

technique makes a significant role in the best study of the dynamics of cultivated land and environmental changes in the study area. Hussain et al. [72] reduced the cotton and rice area by 4.3% and 7.1% in the Multan district during the last 30 years. According to Hussain et al. [73], more than 15% of farmers are food insecure, and most regions are either food insecure or are at their bottom line in Southern Punjab, Pakistan. Our results showed that cultivated areas under wheat and cotton decreased by almost 5.4% and 9.1% from 1984 to 2020, respectively, in the study area.

On the other hand, the study area's building/fallow land increased from 9.1% to 10.2% from 1984 to 2020. In our study, crop rotation showed the order of crops cultivated in the area from 1984 to 2020. Main rotations were shown in the area for autumn–spring maize in fodder (Rabi)-fodder (Kharif) because it has short growing seasons, and farmers can grow three times in the same cropping year.

According to Zhao et al. [74], it was observed that NDVI variation of any crop differs spatially and temporally and thus can be used as a useful tool to study crop growth changes over time in Burkina Faso, West Africa [75,76]. It is also observed by Usman et al. [61]. They stated that the various crops' starting time, as well as crop-cycle length, can be imagined simply from NDVI trends during 2015, as less positive NDVI values (less than 0.1) represent snow, sand, and barren land while 0.1 to 0.2 represent built-up area and different soils in irrigated Indus Basin, Pakistan. In our study, the overall trend of NDVI showed that vegetated areas such as cotton, wheat, rice, and sugarcane had maximum NDVI values, and the non-vegetated areas, such as built-up areas, had minimum NDVI values. Our results also showed a decreasing trend in various crops during the Rabi and Kharif seasons in District Vehari. According to our study, vegetated areas have maximum values of NDVI (greater than 0.4), and built-up areas show fewer NDVI values (0 to 0.2) in District Vehari. The NDVI is also helpful in finding crop distribution patterns in terms of crop production to understand cropping trends better. Seasonal data should be collected from the NDVI time series using thresholds based on the assumption that an event in phenology has begun when NDVI values reach a predetermined threshold. Hussain et al. [73] showed that low temperature was detected at 27.5 °C and the high temperature rose to 28.1 °C during 40 years in District Lodhran. According to Hussain et al. [77], the mean temperature increased from 27.6 °C to 28.5 °C in the Multan region during the last 30 years. To our results, the low temperature was noted as 19.93 °C, and the high temperature rises to 21.17 °C during the Rabi season. The average temperature was calculated from 34.28 °C to 34.54 °C during the Kharif season in District Vehari. In our study, the maximum temperature was detected in urban areas, and the minimum temperature was observed in water bodies and vegetation areas. The average temperature was recorded in the barren and open area [78].

Using Landsat data, Hussain et al. [79] studied a 4.5% rise in settlements and a decrease in vegetation area from 2000 to 2020 in the Okara district of Punjab, Pakistan. According to Khan et al. [80] showed that a vast quantity of grassland and agricultural land in Islamabad, Pakistan, was replaced by barren land from 1993 to 2018 using Landsat images. According to Khan et al. [80] stated that vegetation degradation decreased by 7.17% between 1990 and 2019 in the districts of Mardan and Charsadda, Khyber Pakhtunkhwa (KPK), Pakistan. In this study, barren land and urban development increased by 5.5% and 2.23%, respectively. In contrast, LULC change direction varies with time, geographical location, slope, and altitude. The building/fallow land increased from 9.1% to 10.2% from 1984 to 2020 in the study area. Our results showed that expansion in urban areas occurred probably from 1984 to 2020, depending on the ground level. Migration of the people from rural to urban areas is the main reason for increasing city areas, which increased the strain on natural resources and vegetation cover. Therefore, the LULC changes can be attributed largely to an increased population in rural–urban areas. The agricultural sector mainly focuses on obtaining food for a rising population, so the governmental capacity to support mitigation is lacking.

According to Hussain et al. [81], the highest temperature decreased the duration of rice and cotton crops, and rainfall positively impacted various crops during the Kharif

season [80]. According to [76], the relationship between climate change and major crops showed that the yields of rice and wheat crops are mainly affected by climate change in the District of Multan, Pakistan. Our outcomes presented that wheat positively relates to rainfall and temperature during germination. However, during March and April, temperature and rainfall showed an important negative relationship with wheat production in the study area. Therefore, the temperature harms the rice and cotton during the Kharif season, but rainfall positively affects rice and cotton production in the study area. Climate change, having a great variability with huge impacts on agriculture, is projected to manifest through changes in water management, for example, especially variation in intensity and frequency of flooding, plant diseases, livestock, water shortage, and less crop production that directly causes decreases in the income of rural farmers.

## 5. Conclusions

The present research studied the relationship of temperature and precipitation with major crops in District Vehari using RS and GIS tools. The cultivated area under wheat and cotton decreased by almost 5.4% and 9.1% from 1984 to 2020, respectively, in District Vehari. Our results showed that the area with major crop browning decreased from 1984 to 2020 concerning the decreased vegetation cover rate such as NDVI. To our results, the low temperature was noted as 19.93 °C, and the high temperature rises to 21.17 °C during the Rabi season. According to our results, the average temperature increased from 34.2 °C to 34.5 °C in District Vehari from 1984 to 2020. According to our study, vegetated areas have maximum values of NDVI (greater than 0.4), and built-up areas show fewer NDVI values (0 to 0.2) in District Vehari. Climate change has positive relation between rainfall with wheat and negative relation of temperature with wheat in District Vehari. Therefore, the temperature harms the rice and cotton during the Kharif season. However, rainfall has a positive relation impact on rice and cotton in the study area. Climatic situations influence different crops; growing cotton and wheat crops were very much changed in the District Vehari from growing regions. Our outcomes recommended that changes in rainfall and temperature had an extreme effect on major crops related to rainfall for all vegetation types. This is deemed necessary for supporting the study of crop management and future planning for the region's farmers. Agricultural areas also played an important role in maintaining the vegetation cover in various lands. Due to the importance of vegetation cover, there is an essential need for a suitable policy in the management of climate change and the ecosystem in Southern Punjab. Our outcomes suggest that the relation of vegetation cover with climate change could help as a model for future environmental improvement and vegetation restoration in regions with similar characteristics.

**Author Contributions:** Conceptualization: S.H., W.N. and A.T.; methodology, M.M., S.H., A.R., S.Q. and A.T.; formal analysis, M.A.B., S.F., F.M. B.G.M., S.Q. and W.N.; writing—original draft preparation, M.A.B., S.F., H.G.A., W.N., S.Q., M.A.B., B.G.M. and A.T.; writing—review and editing, M.A.B., S.F., W.N., B.G.M., M.A., S.Q. and A.T.; supervision, A.T. and funding acquisition, S.Q. All authors have read and agreed to the published version of the manuscript.

**Funding:** The research is financially supported by the National Natural Science Foundation of China (52209068), Postdoctoral Research Foundation of China (2020M682477), and the Fundamental Research Funds for the Central Universities (2042021kf0053).

**Institutional Review Board Statement:** Not applicable.

**Informed Consent Statement:** Not applicable.

**Data Availability Statement:** The datasets used and/or analyzed during the current study are available in the article/from the corresponding author on request.

**Conflicts of Interest:** The authors declare no conflict of interest.

## References

1. Al-Najjar, H.A.H.; Kalantar, B.; Pradhan, B.; Saeidi, V.; Halin, A.A.; Ueda, N.; Mansor, S. Land cover classification from fused DSM and UAV images using convolutional neural networks. *Remote Sens.* **2019**, *11*, 1461. [\[CrossRef\]](#)
2. Abdullahi, S.; Pradhan, B. Land use change modeling and the effect of compact city paradigms: Integration of GIS-based cellular automata and weights-of-evidence techniques. *Environ. Earth Sci.* **2018**, *77*, 1–15. [\[CrossRef\]](#)
3. Pradhan, B.; Al-Najjar, H.A.H.; Sameen, M.I.; Tsang, I.; Alamri, A.M. Unseen land cover classification from high-resolution orthophotos using integration of zero-shot learning and convolutional neural networks. *Remote Sens.* **2020**, *12*, 1676. [\[CrossRef\]](#)
4. Hussain, S.; Mubeen, M.; Sultana, S.R.; Ahmad, A.; Fahad, S.; Nasim, W.; Ahmad, S.; Ali, A.; Farid, H.U.; Javeed, H.M.R.; et al. Managing Greenhouse Gas Emission. In *Modern Techniques of Rice Crop Production*; Sarwar, N., Atique-ur-Rehman, Ahmad, S., Hasanuzzaman, M., Eds.; Springer: Singapore, 2022. [\[CrossRef\]](#)
5. Hoffmann, P.; Krueger, O.; Schlünzen, K.H. A statistical model for the urban heat island and its application to a climate change scenario. *Int. J. Climatol.* **2012**, *32*, 1238–1248. [\[CrossRef\]](#)
6. Siddiqui, S.; Ali Safi, M.W.; Rehman, N.U.; Tariq, A. Impact of Climate Change on Land use/Land cover of Chakwal District. *Int. J. Econ. Environ. Geol.* **2020**, *11*, 65–68. [\[CrossRef\]](#)
7. Shah, S.H.I.A.; Yan, J.; Ullah, I.; Aslam, B.; Tariq, A.; Zhang, L.; Mumtaz, F. Classification of aquifer vulnerability by using the drastic index and geo-electrical techniques. *Water* **2021**, *13*, 2144. [\[CrossRef\]](#)
8. Waleed, M.; Mubeen, M.; Ahmad, A.; Habib-ur-Rahman, M.; Amin, A.; Farid, H.U.; El Sabagh, A. Evaluating the efficiency of coarser to finer resolution multispectral satellites in mapping paddy rice fields using GEE implementation. *Sci. Rep.* **2022**, *12*, 13210. [\[CrossRef\]](#)
9. Tariq, A.; Shu, H.; Siddiqui, S.; Imran, M.; Farhan, M. Monitoring land use and land cover changes using geospatial techniques, a case study of Fateh Jang, Attock, Pakistan. *Geogr. Environ. Sustain.* **2021**, *14*, 41–52. [\[CrossRef\]](#)
10. Akram, R.; Turan, V.; Hammad, H.M.; Ahmad, S.; Hussain, S.; Hasnain, A.; Maqbool, M.M.; Rehmani, M.I.A.; Rasool, A.; Masood, N.; et al. Fate of organic and inorganic pollutants in paddy soils. In *Environment Pollution of Paddy Soils*; Springer: Cham, Switzerland, 2018; pp. 197–214. [\[CrossRef\]](#)
11. Wang, B.; Liu, D.; Liu, S.; Zhang, Y.; Lu, D.; Wang, L. Impacts of urbanization on stream habitats and macroinvertebrate communities in the tributaries of Qiangtang River, China. *Hydrobiologia* **2012**, *680*, 39–51. [\[CrossRef\]](#)
12. Zahoor, S.A.; Ahmad, S.; Ahmad, A.; Wajid, A.; Khaliq, T.; Mubeen, M.; Hussain, S.; Din, M.S.U.; Amin, A.; Awais, M.; et al. Improving Water Use Efficiency in Agronomic Crop Production. In *Agronomic Crops*; Springer: Singapore, 2019; pp. 13–29. [\[CrossRef\]](#)
13. Ahmed, B.; Kamruzzaman, M.D.; Zhu, X.; Shahinoor Rahman, M.D.; Choi, K. Simulating land cover changes and their impacts on land surface temperature in dhaka, bangladesh. *Remote Sens.* **2013**, *5*, 5969–5998. [\[CrossRef\]](#)
14. Akram, R.; Amanet, K.; Iqbal, J.; Fatima, M.; Mubeen, M.; Hussain, S.; Fahad, S. Climate Change, Insects and Global Food Production. In *Climate Change and Ecosystems*; CRC Press: New York, NY, USA, 2022; pp. 47–60.
15. Omran, E.-S.E. Detection of Land-Use and Surface Temperature Change at Different Resolutions. *J. Geogr. Inf. Syst.* **2012**, *4*, 189–203. [\[CrossRef\]](#)
16. Yu, X.; Guo, X.; Wu, Z. Land surface temperature retrieval from landsat 8 TIRS-comparison between radiative transfer equation-based method, split window algorithm and single channel method. *Remote Sens.* **2014**, *6*, 9829–9852. [\[CrossRef\]](#)
17. Mubeen, M.; Bano, A.; Ali, B.; Islam, Z.U.; Ahmad, A.; Hussain, S.; Fahad, S.; Nasim, W. Effect of plant growth promoting bacteria and drought on spring maize (*Zea mays* L.). *Pak. J. Bot.* **2021**, *53*, 731–739. [\[CrossRef\]](#)
18. Hussain, S.; Ahmad, A.; Wajid, A.; Khaliq, T.; Hussain, N.; Mubeen, M.; Farid, H.U.; Imran, M.; Hammad, H.M.; Awais, M.; et al. Irrigation Scheduling for Cotton Cultivation. In *Cotton Production Uses*; Springer: Singapore, 2020; pp. 59–80. [\[CrossRef\]](#)
19. Hussain, S. Land Use/Land Cover Classification by Using Satellite NDVI Tool for Sustainable Water and Climate Change in Southern Punjab. Master's Thesis, COMSATS University Islamabad, Islamabad, Pakistan, 2018. [\[CrossRef\]](#)
20. Bryson, R.A.; Swain, A.M. Holocene variations of monsoon rainfall in Rajasthan. *Quaternary Res.* **1981**, *16*, 135–145. [\[CrossRef\]](#)
21. Asad, F.; Zhu, H.; Zhang, H.; Liang, E.; Muhammad, S.; Farhan, S.B.; Hussain, I.; Atif Wazir, M.; Ahmed, M.; Esper, J. Are Karakoram temperatures out of phase compared to hemispheric trends? *Clim. Dyn.* **2017**, *48*, 3381–3390. [\[CrossRef\]](#)
22. Jan, F.; Schüller, L.; Asad, F.; Behling, H. Vegetation and climate dynamics in Khyber Pakhtunkhwa (NW Pakistan), inferred from the pollen record of the Kabal Valley in Swat District during the last 3300 years. *Acta Palaeobot.* **2019**, *59*, 145–163. [\[CrossRef\]](#)
23. Yadava, A.K.; Bräuning, A.; Singh, J.; Yadav, R.R. Boreal spring precipitation variability in the cold arid western Himalaya during the last millennium, regional linkages, and socio-economic implications. *Quat. Sci. Rev.* **2016**, *144*, 28–43. [\[CrossRef\]](#)
24. Hussain, S.; Mubeen, M.; Ahmad, A.; Fahad, S.; Nasim, W.; Hammad, H.M.; Parveen, S. Using space–time scan statistic for studying the effects of COVID-19 in Punjab, Pakistan: A guideline for policy measures in regional agriculture. *Environ. Sci. Pollut. Res.* **2021**, 1–14. [\[CrossRef\]](#)
25. Baqa, M.F.; Chen, F.; Lu, L.; Qureshi, S.; Tariq, A.; Wang, S.; Jing, L.; Hamza, S.; Li, Q. Monitoring and modeling the patterns and trends of urban growth using urban sprawl matrix and CA-Markov model: A case study of Karachi, Pakistan. *Land* **2021**, *10*, 700. [\[CrossRef\]](#)
26. Hu, P.; Sharifi, A.; Tahir, M.N.; Tariq, A.; Zhang, L.; Mumtaz, F.; Shah, S.H.I.A. Evaluation of Vegetation Indices and Phenological Metrics Using Time-Series MODIS Data for Monitoring Vegetation Change in Punjab, Pakistan. *Water* **2021**, *13*, 2550. [\[CrossRef\]](#)

27. Tariq, A.; Riaz, I.; Ahmad, Z.; Amin, M.; Kausar, R.; Andleeb, S.; Farooqi, M.A.; Rafiq, M. Land surface temperature relation with normalized satellite indices for the estimation of spatio-temporal trends in temperature among various land use land cover classes of an arid Potohar region using Landsat data. *Environ. Earth Sci.* **2020**, *79*, 1–15. [[CrossRef](#)]
28. Sharifi, A.; Mahdipour, H.; Moradi, E.; Tariq, A. Agricultural Field Extraction with Deep Learning Algorithm and Satellite Imagery. *J. Indian Soc. Remote Sens.* **2022**, *50*, 417–423. [[CrossRef](#)]
29. Mumtaz, F.; Tao, Y.; Leeuw, G.D.; Zhao, L.; Fan, C.; Elnashar, A.; Bashir, B.; Wang, G.; Li, L.L.; Naeem, S.; et al. Modeling spatio-temporal land transformation and its associated impacts on land surface temperature (LST). *Remote Sens.* **2020**, *12*, 2987. [[CrossRef](#)]
30. Tariq, A.; Yan, J.; Gagnon, A.S.; Riaz Khan, M.; Mumtaz, F. Mapping of cropland, cropping patterns and crop types by combining optical remote sensing images with decision tree classifier and random forest. *Geo-Spat. Inf. Sci.* **2022**, 1–19. [[CrossRef](#)]
31. Jalayer, S.; Sharifi, A.; Abbasi-Moghadam, D.; Tariq, A.; Qin, S. Modeling and Predicting Land Use Land Cover Spatiotemporal Changes: A Case Study in Chalus Watershed, Iran. *IEEE J. Sel. Top. Appl. Earth Obs. Remote Sens.* **2022**, *15*, 5496–5513. [[CrossRef](#)]
32. Ghaderizadeh, S.; Abbasi-Moghadam, D.; Sharifi, A.; Tariq, A.; Qin, S. Multiscale Dual-Branch Residual Spectral-Spatial Network with Attention for Hyperspectral Image Classification. *IEEE J. Sel. Top. Appl. Earth Obs. Remote Sens.* **2022**, *15*, 5455–5467. [[CrossRef](#)]
33. Wahla, S.S.; Kazmi, J.H.; Sharifi, A.; Shirazi, S.A.; Tariq, A.; Joyell Smith, H. Assessing spatio-temporal mapping and monitoring of climatic variability using SPEI and RF machine learning models. *Geocarto Int.* **2022**, 1–20. [[CrossRef](#)]
34. Majeed, M.; Tariq, A.; Anwar, M.M.; Khan, A.M.; Arshad, F.; Shaukat, S. Monitoring of Land Use–Land Cover Change and Potential Causal Factors of Climate Change in Jhelum District, Punjab, Pakistan, through GIS and Multi-Temporal Satellite Data. *Land* **2021**, *10*, 1026. [[CrossRef](#)]
35. Wang, S.; Ma, Q.; Ding, H.; Liang, H. Detection of urban expansion and land surface temperature change using multi-temporal landsat images. *Resour. Conserv. Recycl.* **2018**, *128*, 526–534. [[CrossRef](#)]
36. Zhang, X.; Wang, D.; Hao, H.; Zhang, F.; Hu, Y. Effects of Land Use/Cover Changes and Urban Forest Configuration on Urban Heat Islands in a Loess Hilly Region: Case Study Based on Yan’an City, China. *Int. J. Environ. Res. Public Health* **2017**, *14*, 840. [[CrossRef](#)]
37. Tran, D.X.; Pla, F.; Latorre-Carmona, P.; Myint, S.W.; Caetano, M.; Kieu, H.V. Characterizing the relationship between land use land cover change and land surface temperature. *ISPRS J. Photogramm. Remote Sens.* **2017**, *124*, 119–132. [[CrossRef](#)]
38. Butt, A.; Shabbir, R.; Ahmad, S.S.; Aziz, N. Land use change mapping and Analysis using Remote Sensing and GIS: A case study of Simly watershed, Islamabad, Pakistan. *Egypt. J. Remote Sens. Sp. Sci.* **2015**, *18*, 251–259. [[CrossRef](#)]
39. Din, M.S.U.; Mubeen, M.; Hussain, S.; Ahmad, A.; Hussain, N.; Ali, M.A.; Nasim, W. World Nations Priorities on Climate Change and Food Security. In *Building Climate Resilience in Agriculture*; Springer: Cham, Switzerland, 2022; pp. 365–384. [[CrossRef](#)]
40. Tariq, A.; Siddiqui, S.; Sharifi, A.; Hassan, S.; Ahmad, I. Impact of spatio-temporal land surface temperature on cropping pattern and land use and land cover changes using satellite imagery, Hafizabad District, Punjab, Province of Pakistan. *Arab. J. Geosci.* **2022**, *15*, 1–16. [[CrossRef](#)]
41. Fu, C.; Cheng, L.; Qin, S.; Tariq, A.; Liu, P.; Zou, K.; Chang, L. Timely Plastic-Mulched Cropland Extraction Method from Complex Mixed Surfaces in Arid Regions. *Remote Sens.* **2022**, *14*, 4051. [[CrossRef](#)]
42. Jahangir, M.; Maria Ali, S.; Khalid, B. Annual minimum temperature variations in early 21st century in Punjab, Pakistan. *J. Atmos. Sol.-Terr. Phys.* **2016**, *137*, 1–9. [[CrossRef](#)]
43. Zereen, A.; Khan, Z. A survey of ethnobotanically important trees of Central Punjab, Pakistan. *Biology* **2012**, *58*, 21–30.
44. Waseem, M.; Khurshid, T.; Abbas, A.; Ahmad, I.; Javed, Z. Impact of meteorological drought on agriculture production at different scales in Punjab, Pakistan. *J. Water Clim. Chang.* **2022**, *13*, 113–124. [[CrossRef](#)]
45. Naz, S.; Fatima, Z.; Iqbal, P.; Khan, A.; Zakir, I.; Ullah, H.; Ahmad, S. An Introduction to Climate Change Phenomenon. In *Building Climate Resilience in Agriculture*; Springer: Cham, Switzerland, 2022; pp. 3–16. [[CrossRef](#)]
46. Masood, N.; Akram, R.; Fatima, M.; Mubeen, M.; Hussain, S.; Shakeel, M.; Nasim, W. Insect Pest Management Under Climate Change. In *Building Climate Resilience in Agriculture*; Springer: Cham, Switzerland, 2022; pp. 225–237. [[CrossRef](#)]
47. Hussain, S.; Amin, A.; Mubeen, M.; Khaliq, T.; Shahid, M.; Hammad, H.M.; Nasim, W. Climate Smart Agriculture (CSA) Technologies. In *Building Climate Resilience in Agriculture*; Springer: Cham, Switzerland, 2022; pp. 319–338. [[CrossRef](#)]
48. Tariq, A.; Mumtaz, F.; Zeng, X.; Baloch, M.Y.J.; Moazzam, M.F.U. Spatio-temporal variation of seasonal heat islands mapping of Pakistan during 2000–2019, using day-time and night-time land surface temperatures MODIS and meteorological stations data. *Remote Sens. Appl. Soc. Environ.* **2022**, *27*, 100779. [[CrossRef](#)]
49. Nasim, W.; Amin, A.; Fahad, S.; Awais, M.; Khan, N.; Mubeen, M.; Hussain, S. Future risk assessment by estimating historical heat wave trends with projected heat accumulation using SimCLIM climate model in Pakistan. *Atmos. Res.* **2018**, *205*, 118–133. [[CrossRef](#)]
50. Hassan, Z.; Shabbir, R.; Ahmad, S.S.; Malik, A.H.; Aziz, N.; Butt, A.; Erum, S. Dynamics of land use and land cover change (LULCC) using geospatial techniques: A case study of Islamabad Pakistan. *Springerplus* **2016**, *5*, 812. [[CrossRef](#)]
51. Islam, M.S.; Fahad, S.; Hossain, A.; Chowdhury, M.K.; Iqbal, M.A.; Dubey, A.; Sabagh, A.E. Legumes under Drought Stress: Plant Responses, Adaptive Mechanisms, and Management Strategies in Relation to Nitrogen Fixation. In *Engineering Tolerance in Crop Plants Against Abiotic Stress*; CRC Press: New York, NY, USA, 2021; pp. 179–207.



52. Abbas, F.; Sarwar, N.; Ibrahim, M.; Adrees, M.; Ali, S.; Saleem, F.; Hammad, H.M. Patterns of Climate Extremes in the Coastal and Highland Regions of Balochistan, Pakistan. *Earth Interact.* **2018**, *22*, 1–23. [[CrossRef](#)]
53. Ur Rehman, Z.; Kazmi, S.J.H. Land use/land cover changes through satellite remote sensing approach: A case study of Indus delta, Pakistan. *Pakistan J. Sci. Ind. Res. Ser. A Phys. Sci.* **2018**, *61*, 156–162. [[CrossRef](#)]
54. Abid, M.; Schilling, J.; Scheffran, J.; Zulfiqar, F. Climate change vulnerability, adaptation and risk perceptions at farm level in Punjab, Pakistan. *Sci. Total Environ.* **2016**, *547*, 447–460. [[CrossRef](#)]
55. Aslam, A.Q.; Ahmad, S.R.; Ahmad, I.; Hussain, Y.; Hussain, M.S. Vulnerability and impact assessment of extreme climatic event: A case study of southern Punjab, Pakistan. *Sci. Environ.* **2017**, *580*, 468–481. [[CrossRef](#)]
56. Aslam, A.Q.; Ahmad, I.; Ahmad, S.R.; Hussain, Y.; Hussain, M.S.; Shamshad, J.; Zaidi, S.J.A. Integrated climate change risk assessment and evaluation of adaptation perspective in southern Punjab, Pakistan. *Sci. Total Environ.* **2018**, *628–629*, 1422–1436. [[CrossRef](#)] [[PubMed](#)]
57. Ahmed, K.; Shahid, S.; Nawaz, N. Impacts of climate variability and change on seasonal drought characteristics of Pakistan. *Atmos. Res.* **2018**, *214*, 364–374. [[CrossRef](#)]
58. Amin, A.; Nasim, W.; Fahad, S.; Ali, S.; Ahmad, S.; Rasool, A.; Saleem, N.; Hammad, H.M.; Sultana, S.R.; Mubeen, M.; et al. Evaluation and Analysis of temperature for historical (1996–2015) and projected (2030–2060) climates in Pakistan using SimCLIM climate model: Ensemble application. *Atmos. Res.* **2018**, *213*, 422–436. [[CrossRef](#)]
59. Amin, A.; Nasim, W.; Mubeen, M.; Sarwar, S.; Urich, P.; Ahmad, A.; Ali, Q.S. Regional climate assessment of precipitation and temperature in Southern Punjab (Pakistan) using SimCLIM climate model for different temporal scales. *Theor. Appl. Climatol.* **2018**, *131*, 121–131. [[CrossRef](#)]
60. Usman, U.; Yelwa, S.A.; Gulumbe, S.U.; Danbaba, A.; Nir, R. Modelling Relationship between NDVI and Climatic Variables Using Geographically Weighted Regression. *J. Math. Sci. Appl.* **2013**, *1*, 24–28. [[CrossRef](#)]
61. Campo-Bescós, M.A.; Muñoz-Carpena, R.; Southworth, J.; Zhu, L.; Waylen, P.R.; Bunting, E. Combined spatial and temporal effects of environmental controls on long-term monthly NDVI in the Southern Africa Savanna. *Remote Sens.* **2013**, *5*, 6513–6538. [[CrossRef](#)]
62. Fazal, S. Urban expansion and loss of agricultural land—A GIS based study of Saharanpur City, India. *Environ. Urban.* **2000**, *12*, 133–149. [[CrossRef](#)]
63. Aguilár, A.G.; Ward, P.M. Globalization, regional development, and mega-city expansion in Latin America: Analyzing Mexico City’s peri-urban hinterland. *Cities* **2003**, *20*, 3–21. [[CrossRef](#)]
64. Athick, A.A.S.M.; Shankar, K. Data on Land Use and Land Cover Changes in Adama Wereda, Ethiopia, on ETM+, TM and OLI-TIRS landsat sensor using PCC and CDM techniques. *Data Brief* **2019**, *24*, 103880. [[CrossRef](#)] [[PubMed](#)]
65. Tariq, A.; Shu, H. CA-Markov Chain Analysis of Seasonal Land Surface Temperature and Land Use Landcover Change Using Optical Multi-Temporal Satellite Data of. *Remote Sens.* **2020**, *12*, 3402. [[CrossRef](#)]
66. Sayemuzzaman, M.; Jha, M.K. Modeling of Future Land Cover Land Use Change in North Carolina Using Markov Chain and Cellular Automata Model. *Am. J. Eng. Appl. Sci.* **2014**, *7*, 295–306. [[CrossRef](#)]
67. Zhang, Q.; Wang, J.; Peng, X.; Gong, P.; Shi, P. Urban built-up land change detection with road density and spectral information from multi-temporal Landsat TM data. *Int. J. Remote Sens.* **2002**, *23*, 3057–3078. [[CrossRef](#)]
68. Hussain, S.; Mubeen, M.; Ahmad, A.; Majeed, H.; Qaisrani, S.A.; Hammad, H.M.; Nasim, W. Assessment of land use/land cover changes and its effect on land surface temperature using remote sensing techniques in Southern Punjab, Pakistan. *Environ. Sci. Pollut. Res.* **2022**, 1–17. [[CrossRef](#)] [[PubMed](#)]
69. Chen, W.; Liu, L.; Zhang, C.; Wang, J.; Wang, J.; Pan, Y. Monitoring the seasonal bare soil areas in Beijing using multitemporal TM images. In Proceedings of the IGARSS 2004, 2004 IEEE International Geoscience and Remote Sensing Symposium, Anchorage, AL, USA, 20–24 September 2004; Volume 5, pp. 3379–3382.
70. Ahmed, B.; Ahmed, R. Modeling urban land cover growth dynamics using multioral satellite images: A case study of Dhaka, Bangladesh. *ISPRS Int. J. Geo-Inf.* **2012**, *1*, 3–31. [[CrossRef](#)]
71. Hussain, S.; Mubeen, M.; Akram, W.; Ahmad, A.; Habib-ur-Rahman, M.; Ghaffar, A.; Amin, A.; Awais, M.; Farid, H.U.; Farooq, A.; et al. Study of land cover/land use changes using RS and GIS: A case study of Multan district, Pakistan. *Environ. Monit. Assess.* **2020**, *192*, 2. [[CrossRef](#)]
72. Hussain, S.; Mubeen, M.; Ahmad, A.; Akram, W.; Hammad, H.M.; Ali, M.; Masood, N.; Amin, A.; Farid, H.U.; Sultana, S.R.; et al. Using GIS tools to detect the land use/land cover changes during forty years in Lodhran District of Pakistan. *Environ. Sci. Pollut. Res.* **2020**, *27*, 39676–39692. [[CrossRef](#)]
73. Zhao, Z.; Sharifi, A.; Dong, X.; Shen, L.; He, B.J. Spatial Variability and Temporal Heterogeneity of Surface Urban Heat Island Patterns and the Suitability of Local Climate Zones for Land Surface Temperature Characterization. *Remote Sens.* **2021**, *13*, 4338. [[CrossRef](#)]
74. Talukdar, S.; Rihan, M.; Hang, H.T.; Bhaskaran, S.; Rahman, A. Modelling urban heat island (UHI) and thermal field variation and their relationship with land use indices over Delhi and Mumbai metro cities. *Environ. Dev. Sustain.* **2021**, *24*, 3762–3790.
75. Sharma, R.; Pradhan, L.; Kumari, M.; Bhattacharya, P. Assessing urban heat islands and thermal comfort in Noida City using geospatial technology. *Urban Clim.* **2021**, *35*, 100751. [[CrossRef](#)]

76. Hussain, S.; Mubeen, M.; Ahmad, A.; Masood, N.; Hammad, H.M.; Amjad, M.; Waleed, M. Satellite-based evaluation of temporal change in cultivated land in Southern Punjab (Multan region) through dynamics of vegetation and land surface temperature. *Open Geosci.* **2021**, *13*, 1561–1577. [[CrossRef](#)]
77. Hussain, S.; Karuppannan, S. Land use/land cover changes and their impact on land surface temperature using remote sensing technique in district Khanewal, Punjab Pakistan. *Geol. Eco. Landsc.* **2021**, 1–13. [[CrossRef](#)]
78. Hussain, S.; Mubeen, M.; Karuppannan, S. Land use and land cover (LULC) change analysis using TM, ETM+ and OLI Landsat images in district of Okara, Punjab, Pakistan. *Phys. Chem. Earth Parts A/B/C* **2022**, *126*, 103117. [[CrossRef](#)]
79. Khan, R.; Li, H.; Basir, M.; Chen, Y.L.; Sajjad, M.M.; Haq, I.U.; Hassan, W. Monitoring land use land cover changes and its impacts on land surface temperature over Mardan and Charsadda Districts, Khyber Pakhtunkhwa (KP), Pakistan. *Environ. Monit. Assess.* **2022**, *194*, 1–22. [[CrossRef](#)]
80. Khan, M.S.; Ullah, S.; Sun, T.; Rehman, A.U.; Chen, L. Land-Use/Land-Cover Changes and Its Contribution to Urban Heat Island: A Case Study of Islamabad, Pakistan. *Sustainability* **2020**, *12*, 3861. [[CrossRef](#)]
81. Hussain, S.; Lu, L.; Mubeen, M.; Nasim, W.; Karuppannan, S.; Fahad, S.; Aslam, M. Spatiotemporal Variation in Land Use Land Cover in the Response to Local Climate Change Using Multispectral Remote Sensing Data. *Land* **2022**, *11*, 595. [[CrossRef](#)]